Wang, J., Hinck, A. P., Loh, S. N., & Markley, J. L. (1990) *Biochemistry 29*, 102–113.
Wingfield, P. T., Payton, M., Tavernier, J., Barnes, M., Shaw, A., Rose, K., Simona, M. G., Demaczuk, S., Williamson, K., & Dayer, J.-M. (1986) *Eur. J. Biochem. 160*, 491–497.
Wüthrich, K. (1986) *NMR of Proteins and Nucleic Acids*, Wiley, New York.
Wüthrich, K. (1989) *Acc. Chem. Res. 22*, 36–44.
Zuiderweg, E. R. P., McIntosh, L. P., Dahlquist, F. W., & Fesik, S. W. (1990) *J. Magn. Reson. 86*, 210–216.

# Study of the Binding of Single-Stranded DNA-Binding Protein to DNA and Poly(rA) Using Electric Field Induced Birefringence and Circular Dichroism Spectroscopy†

M. E. Kuil,*,‡ K. Holmlund,§ C. A. Vlaanderen, and R. van Grondelle
*Department of Physics and Astronomy, Free University de Boelelaan 1081, 1081 HV Amsterdam, The Netherlands*
*Received November 9, 1989; Revised Manuscript Received March 28, 1990*

ABSTRACT: Binding of the single-stranded DNA-binding protein (SSB) of *Escherichia coli* to single-stranded (ss) polynucleotides produces characteristic changes in the absorbance (OD) and circular dichroism (CD) spectra of the polynucleotides. By use of these techniques, complexes of SSB protein and poly(rA) were shown to display two of the binding modes reported by Lohman and Overman [Lohman, T. M., & Overman, L. (1985) *J. Biol. Chem. 260*, 3594–3603]. The circular dichroism spectra of the "low salt" (10 mM NaCl) and "high salt" (>50 mM NaCl) binding mode are similar in shape, but not in intensity. SSB binding to poly(rA) yields a complexed CD spectrum that shares several characteristics with the spectra obtained for the binding of AdDBP, GP32, and gene V protein to poly(rA). We therefore propose that the local structure of the SSB–poly(rA) complex is comparable to the structures proposed for the complexes of these three-stranded DNA-binding proteins with DNA (and RNA) and independent of the SSB-binding mode. Electric field induced birefringence experiments were used to show that the projected base–base distance of the complex is about 0.23 nm, in agreement with electron microscopy results. Nevertheless, the local distance between the successive bases in the complex will be quite large, due to the coiling of the DNA around the SSB tetramer, thus partly explaining the observed CD changes induced upon complexation with single-stranded DNA and RNA.

The binding properties of *Escherichia coli* SSB protein, belonging to the class of single-stranded DNA-binding proteins, show many similarities with the properties of gene 32 protein and AdDBP, the single-stranded DNA-binding protein of the (eukaryotic) adenovirus [for a review, see Chase and Williams (1986)]. Only recently the rather different binding properties of the SSB protein, as compared to GP32 and AdDBP, were fully recognized by Lohman and co-workers (Lohman & Overman, 1985; Bujalowski & Lohman, 1986; Bujalowski et al., 1988). A comprehensive review covering this subject appeared recently (Lohman et al., 1988). The variety of binding modes exhibited by SSB protein depend on the salt concentration, salt type, pH, and temperature and are characterized by a different size of the binding site. Moreover, is was shown that the binding of the protein can be described more accurately assuming the "nearest neighbor cooperativity" model (McGhee & von Hippel, 1974) that successfully explained the binding properties of GP32 [see Kowalczykowski et al. (1986) and references cited therein] and recently also the binding of AdDBP to poly(rA) (Kuil et al., 1989).

The SSB protein is a multifunctional protein in the DNA metabolism of *E. coli*; it is essential for DNA replication, DNA recombination, and repair (Chase & Williams, 1986). Moreover, the protein protects the single-stranded DNA against nuclease activity. The variety of functions that the SSB protein plays in the cell may well be related to the observed different binding modes in vitro as well as to the interaction of SSB with several *E. coli* proteins [recA, pol II, exoI, and the n protein (Morrical et al., 1986; Sigal et al., 1972; Molineux & Gefter, 1975; Low et al., 1982)]. As an example, recent experiments of Kowalczykowski et al. (Kowalczykowski et al., 1987; Kowalczykowski & Krupp, 1987) have shown that the effect of the SSB protein on the ATPase activity of *E. coli* recA protein is critically dependent on the temperature, the substrate, the order of addition, and the magnesium concentration. It was shown by Kowalczykowski et al. that either the SSB protein displaces the recA protein from the single-stranded DNA or recA is able to displace the SSB protein, dependent on the presence of cofactors. In previous studies, we reported the solution dimensions of complexes of GP32 and ssDNA fragments using electric birefringence and quasi-elastic light-scattering experiments. For GP32, it was observed that the projected distance between the DNA bases increased substantially (0.53 nm compared to 0.34 nm per base for double-stranded DNA) (Scheerhagen et al., 1985a,b; Scheerhagen, 1986; Kuil et al., 1990). Moreover, it was shown that the complex has a low bending persistence length of about 35 nm (Kuil et al., 1988, 1990). An increase of the base–base distance to 0.47 nm was observed by Delius using electron microscopy for GP32 binding to fd DNA (Delius et al., 1972). For SSB, similar electron microscopy experiments were performed, indicative of a decreased base–base distance of 0.19 nm per base (using a value of 6407 nucleotides in the fd DNA)

† Supported by the Dutch Organization of Pure Research (NWO) via the Foundation of Biophysics (Stichting voor Biofysica).
‡ Present address: Department of Physical and Macromolecular Chemistry, Gorlaeus Laboratories, POB 9502, 2300 RA Leiden, The Netherlands.
§ Present address: Institute of Theoretical Physics, Chalmers University of Technology, University of Göteborg, S-41296 Göteborg, Sweden.

0006-2960/90/0429-8184$02.50/0 

(Sigal et al., 1972), and supercoiling or some other regularly folded structure of the complex was proposed. The actual distance between the bases in the SSB complexes will be larger due to this supercoiling. The model for the structure of the SSB-binding modes proposed by Lohman et al. assumes that the DNA is wrapped around a tetramer or an octamer (dimer of two tetramers) dependent on the actual binding mode (Lohman et al., 1985). In this work, we determined the hydrodynamic dimensions of a SSB complex with small single-stranded DNA fragments using electric birefringence experiments, assuming that the diameter of the complex is 7.6 nm, corresponding to the Stokes diameter of the SSB tetramer (Weiner et al., 1975; Bandyopadhyay & Wu, 1978). The obtained dimensions depend furthermore on the assumed shape of the particle and on the flexibility of the particle (Kuil et al., 1990). Assuming a rigid cylindrical shape for the complex, we find the projected base–base distance is 0.23 ± 0.03 nm, in reasonable agreement with the earlier electron microscopy results (Sigal et al., 1972). Furthermore, we have studied the structure of the DNA in the complex, using CD spectroscopy, and we interpret the data in terms of the results obtained by Scheerhagen et al. (Scheerhagen et al., 1986; Scheerhagen, 1986) and van Amerongen et al. (van Amerongen et al., 1987; van Amerongen, 1989). To explain the observed changes in the CD spectra of poly(rA) upon complexation with SSB, we postulate that the local structure of the complex must very similar to that of GP32, gene V protein, the single-stranded DNA-binding protein coded by the DNA of the bacteriophages fd and M13, and AdDBP protein, all complexed with poly(rA) (Anderson & Coleman, 1975; van Amerongen et al., 1987). These structures are characterized by an increased base–base distance, a substantial tilt of the bases, a low rotation per base, and/or a positioning of the bases close to the local helix axis in the complex (Scheerhagen et al., 1986, 1989; van Amerongen et al., 1988; van Amerongen, 1989).

## Materials and Methods

The SSB protein was purified from *E. coli* strain CS 4791 containing the plasmids pPLssb and pCI (Brandsma et al., 1981), essentially as described by Lohman et al. (1986). SDS gel electrophoresis followed by silver staining showed that the protein was more than 98% pure. At low salt strength, the Bradford reagent (Bradford, 1976) was used to determine the SSB concentration since the UV absorbance measurements were unreliable due to strong light scattering. The Bradford method was compared with the concentration as determined by UV absorbance in buffer TE + 200 mM NaCl. Both methods agreed within 5% when an extinction coefficient of $\epsilon_{280}$ = 113 000 $M^{-1}$ $cm^{-1}$ (tetramers) (Lohman & Overman, 1985) and a molecular weight of 18 873 for the SSB monomer were used. Double-stranded DNA fragments containing 145 base pairs were isolated from chicken erythrocytes according to the method described by Lutter (1978). Details of the preparation of the 270 bp DNA fragment and the determination of the size of this fragment, both using electric field induced birefringence experiments and polyacrylamide gel electrophoresis, are given by Kuil et al. (1990). Poly(rA) was obtained from Pharmacia (Woerden, The Netherlands). The standard buffer for all experiments was buffer TE, containing 10 mM Tris-HCl and 0.1 mM $Na_2EDTA$, pH 8.1 ($T$ = 20 °C), together with the indicated NaCl concentration. The dsDNA fragments were denatured prior to the experiment, and the DNA–protein complexes were prepared as described before (Scheerhagen, 1986, Kuil et al., 1990). The following extinction coefficients were used to determine spectrophotometrically the concentrations of the nucleotides: ss 145 bp DNA, ss 270 bp DNA, $\epsilon_{260}$ = 7920 $M^{-1}$ $cm^{-1}$; poly(rA), $\epsilon_{260}$ = 9400 $M^{-1}$ $cm^{-1}$. CD spectra were recorded on a Cary 61 spectropolarimeter, which was extensively modified (Bokma et al., 1987). The electric birefringence setup is essentially the same as described by Greve with some modifications reported by Scheerhagen (Greve, 1972; Scheerhagen, 1986). The experiment was interfaced to a HP85 computer that controlled the experiment and stored the collected data on tape. Data analysis was performed on a VME131 or SUN4 computer system using a Marquardt algorithm for the nonlinear least-squares fits (Marquardt, 1963). All reported decay times and diffusion coefficients were obtained at temperatures close to 12 °C and corrected to a standard temperature of 20 °C.

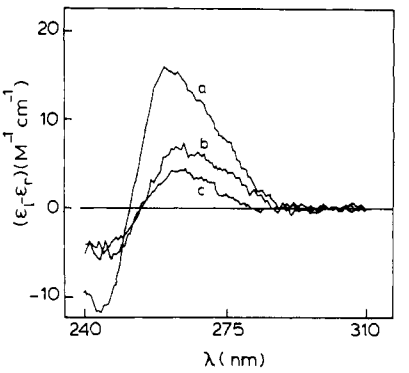


FIGURE 1: CD spectra of SSB protein complexed with poly(rA). Spectrum a: uncomplexed poly(rA). Spectrum b: SSB bound to poly(rA) in the $n$ = 65 binding mode; TE buffer containing 50 mM NaCl. Spectrum c: SSB bound to poly(rA) in the $n$ = 35 binding mode; TE buffer containing 10 mM NaCl.

## Results

*Structural Information: CD Spectroscopy.* The intensity of the 240–300-nm CD spectrum of single-stranded polynucleotides and natural DNA was shown to decrease upon complexation with SSB protein (Anderson & Coleman, 1975). Figure 1 shows typical CD spectra of uncomplexed poly(rA) and poly(rA) with SSB protein. This experiment was performed in 10 mM NaCl, a condition which favors the low salt binding mode of the SSB protein. The change in the CD spectrum of poly(rA) due to the binding of SSB is rather typical for all of the single-stranded DNA-binding proteins. Titration of the induced CD change at 260 nm versus the protein polynucleotide ratio is shown in Figure 2b. Although there is some scatter, the breakpoint in the titration is observed at an apparent size of the binding site ($n$) of 37 nucleotides covered by an SSB tetramer, confirming that the protein binds under these conditions in the $n$ = 35 or low-salt binding mode. The deviation from stoichiometric binding indicates that the product $K\omega$ is not extremely large at 10 mM NaCl (McGhee & von Hippel, 1974). At this low salt concentration, the protein solutions show a slight scattering, probably due to aggregation of the protein. However, after addition of DNA, the scattering disappears completely. When the NaCl concentration is raised to 50 mM NaCl, the titration curves reveal SSB binding in the $n$ = 65 or high salt binding mode (see Figure 2a) in agreement with the observations of Lohman and Overman (1985). The SSB binding is accompanied, both for high and for low salt concentrations, by very similar changes in the CD spectra (Figure 1). In both binding modes, the positive CD band of poly(rA) is reduced in intensity, whereas the largest changes occur when the protein is bound in the $n$ = 35 mode. The spectral changes in both the $n$ = 35 and the $n$ = 65 mode have more or less the same shape, indicative of a similar local poly(rA) conformation in both complexes.

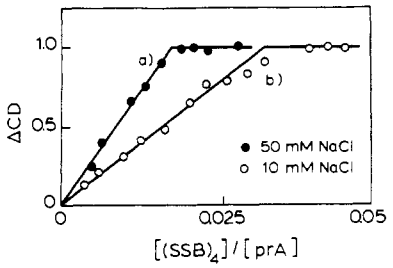


FIGURE 2: Titrations of poly(rA) with SSB protein. The binding of the SSB protein was monitored by using the induced CD change at 260 nm. The CD signal was averaged for several minutes. The induced change compared to the maximum change in an experiment is a measure for the saturation of poly(rA) with SSB protein. The experiments were performed in TE + 10 mM NaCl (open circles) and in TE + 50 mM (closed circles) and resulted in a size for the binding site of 37 ± 4 and 63 ± 5 nucleotides covered by 1 tetramer, respectively.

Similar spectral changes were observed upon binding of GP32, gene V protein, and the AdDBP protein to poly(rA) (Anderson & Coleman, 1975; Scheerhagen, 1986; van Amerongen et al., 1987). These spectral changes can be interpreted as an indication for an increased base–base distance and a substantial tilt of the bases in the complex (Scheerhagen et al., 1986; van Amerongen et al., 1987). For the GP32–poly(rA) complex, these features were indeed observed. We performed identical CD-binding experiments with the 145 and 270 bp DNA fragments. The changes induced in the CD spectra are now rather small, since the signal of single-stranded DNA alone is much smaller than the CD signal from poly(rA) (see Figure 3a). Nevertheless, qualitatively the same changes occur when the SSB protein is bound to the DNA: the positive CD band of the nucleotides is reduced substantially. In 10 mM NaCl + TE, the $n = 35$ binding mode is manifested (see Figure 3b).

From the induced CD changes at 260 nm, we calculated the binding stoichiometry for poly(rA) and the two single-stranded DNA fragments in buffer TE + 10 mM NaCl. For the binding of SSB to poly(rA), we calculated an apparent binding site size of 37 ± 4, while for both ssDNA fragments a stoichiometry of 36 ± 4 nucleotides per tetramer was found. In 50 mM NaCl + TE, an apparent size of the binding site of 63 ± 5 was calculated for the binding of the SSB protein to poly(rA). We note that these values compare very well with those reported by Lohman et al. at comparable salt strengths (Lohman & Overman, 1985). Although the former authors did not report the size of the binding site for SSB bound to poly(rA), they do give the size of the binding site for M13 single-stranded DNA for the two binding modes.

However, it should be noted that the shape of the induced CD change changes slightly between these two binding modes, probably reflecting a slightly different local structure of the poly(rA). If both in the $n = 65$ mode and in the $n = 35$ mode the ss poly(rA) is fully occupied by the SSB and the local structure of these complexes is similar, we expect that the amplitude of the induced CD signal is equal for both binding modes. Assuming a similar conformation of the complex in both binding modes, it can be calculated that about 25% of the poly(rA) is not interacting with SSB in the $n = 65$ mode. Lohman and Overman reported a fluorescence quenching for the two binding modes of SSB to poly(dT) of 51 ± 3 and 83 ± 3% for $n = 33 \pm 3$ and $n = 65 \pm 5$, respectively (Lohman & Overman, 1975). In these measurements, the larger induced change also seems to be related to the number of interactions per tetramer. If we assume that quenching is due to the close association with only 75% of the nucleotides involved in the binding, while in the $n = 33$ mode all nucleotides contribute,

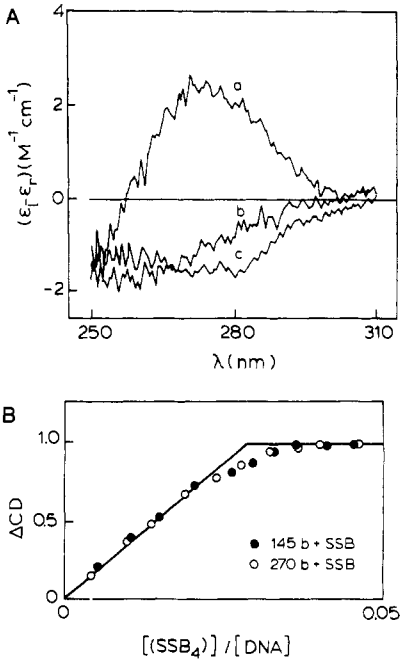


FIGURE 3: (A) CD spectra of SSB protein complexed with short single-stranded DNA fragments. (a) ss 270 bp DNA [60 mM]. (b) ss 270 bp DNA saturated with SSB. (c) ss 145 bp DNA saturated with SSB. The spectra are corrected for dilution and corrected for the protein contribution. (B) Titrations of stranded DNA fragments with SSB protein. The binding of the SSB protein was monitored by using the induced CD change at 272 nm. The open circles represent data points obtained for the 145 bp DNA–SSB complex; the closed circles represent data points obtained for the 270 bp DNA–SSB complex. Buffer TE + 10 nM NaCl was used in both experiments.

then the ratio of the fluorescence quenching of these modes should be about 1.5, quite close to the reported value of 1.6.

*Structural Information: Electric Birefringence.* Electron microscope photographs of the SSB protein complexed with fd DNA show that the contour length of the DNA is reduced to 0.19 nm per base when SSB is bound (Sigal et al., 1972). It was also noted by Sigal et al. that the true value of the contour length can be much higher if the DNA–protein complex is organized in a superhelical structure. Electric field induced birefringence experiments can yield rather accurate estimates of the solution dimensions (notably the length) of suspended macromolecules if the approximate shape of the molecule is known. The rotation diffusion coefficient of a particle is largely determined by the largest dimension of the particle and can be accurately determined from the observed electric field induced birefringence decay. Unfortunately, the technique is limited to solutions with a low salt concentration since conducting samples are heated too much by the applied electric field. The SSB–DNA complexes used for the electric field induced birefringence experiments were prepared by mixing an aliquot of SSB in 10 mM NaCl + TE with the DNA solution in buffer TE without additional salt. The salt concentration that could be used for these experiments ranged from 2 mM NaCl to 10 mM NaCl + TE, and it was confirmed by CD titration experiments that the SSB was bound in the $n = 35$ binding mode to the DNA (see Figure 3b). For uncomplexed single-stranded DNA, a very small positive and fast birefringence signal is observed as reported by Scheerhagen et al. (1986). When the SSB protein is added to the single-stranded DNA, the signal increases significantly as observed before for GP32 (Scheerhagen et al., 1985). This large increase in the observed signal is most likely due to the stiffening of the complex, resulting in a more extended configuration when compared to the uncomplexed single-stranded

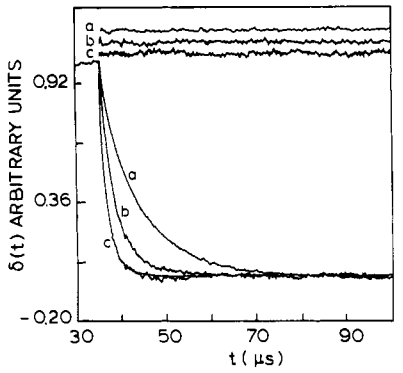


FIGURE 4: Normalized decay of the observed electric birefringence signal for two small single-stranded DNA fragments complexed with SSB protein. Curve a: decay of the birefringence signal for double-stranded 270 bp DNA shown for comparison. Curve b: decay of the birefringence signal for the 270 bp DNA–SSB complex. Curve c: decay of the birefringence signal for the 145 bp DNA–SSB complex. [DNA] = 75 μM, $[(SSB)_4]$ = 2 μM. The residuals from a double-exponential fit are shown at the top of the figure, indicated as a–c. The curves shown are the result of averaging 10–20 individual traces. The best-fit parameters are summarized in Table I.

Table I: Relaxation Times Obtained from the Field-Free Decay of the Electric Field Induced Birefringence Signal

| substrate used | [NaCl] (mM) | $\tau_f$ (μs) | $\tau_s$ (μs) | fraction of the fast component (%) |
|---|---|---|---|---|
| 145 bp DNA | 2–10 | 0.3 ± 0.1 | 1.60 ± 0.15 | 30 ± 10 |
| 270 bp DNA | 2–10 | 0.8 ± 0.2 | 5.77 ± 0.34 | 30 ± 10 |

DNA. Moreover, the decay of the signal, observed when the applied field is switched off, is slower than for the single-stranded DNA alone, again indicative for a more extended structure. When the calculated slowest decay time from a double-exponential fit to the data obtained for the SSB–DNA complex is compared with the native double-stranded DNA of the same length, the length of the SSB complex must be reduced since the decay is faster than for double-stranded DNA alone. This observation, shown in Figure 4, was made for both the 145 bp and the 270 bp SSB–protein complex. In this figure, the normalized birefringence decays of double-stranded 270 bp DNA (a), the 270 bp DNA–SSB complex (b), and the 145 bp DNA–SSB complex (c) can be compared. For the two DNA proteins, we show the residuals of a double-exponential fit at the top of Figure 4. Note that the sign of the birefringence signal is cancelled by the normalization, e.g., the negative birefringence signal for double-stranded DNA is now displayed as a positive signal. The CD spectra recorded before and after the electric birefringence experiment were identical, and in agreement with the spectra shown above. The results of a two-exponential fit of the electric field induced birefringence decays are given in Table I. Typically, the amplitude of the fast component was 30% of the slow amplitude. No dependencies on the pulse height and pulse duration of the calculated parameters could be observed. The experiments were performed in buffers containing different NaCl concentrations (between 2 and 10 mM) without observing changes in the decay times or relative amplitudes of the two decay components. The amplitude of the signal decreases when the salt concentration is increased, and, therefore, the most accurate measurements could be performed at 2 mM NaCl. A major drawback of this low salt strength is the more frequent observation of a positive residual birefringence signal that interferes with the parameter estimation. If the ionic strength was lowered even further, irreproducible results were obtained. The same applies for complexes that were prepared

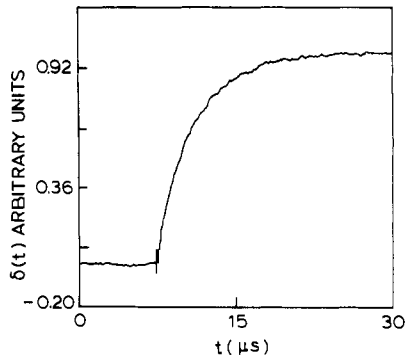


FIGURE 5: Normalized rise of the observed electric birefringence signal for a 270-base DNA fragment complexed with SSB protein. The rise of the birefringence signal can be described rather well with a single exponential (not shown), indicating that there is no significant contribution from a permanent dipole moment in the orientation of the complex.

at a higher NaCl concentration and subsequently dialyzed to reach a low salt strength. Therefore, we diluted complexes prepared in 10 mM NaCl + TE using the TE buffer without additional NaCl, and in this way, samples were prepared that could successfully be used in the electric field induced birefringence experiments. The positive birefringence observed for gene 32 protein complexed with short DNA and tRNA fragments by Scheerhagen et al. (Scheerhagen et al., 1985a, Scheerhagen, 1986) was explained by assuming a substantial tilt of the bases in the GP32–DNA complex. The SSB–ssDNA complexes show a similar positive birefringence signal, albeit somewhat smaller than the signal that is obtained for the ssDNA–GP32 complexes studied earlier (Scheerhagen et al., 1985a; Kuil et al., 1990). Since the electric polarizability of these complexes is roughly proportional to the length squared of the molecule, we assume that this amplitude difference reflects the fact the length of the GP32 complex is more than twice the length of the SSB complex when the same length of DNA is used to form the complex (see below).

The shape of the birefringence curve of the SSB–ssDNA complex shown in Figure 5 is different from the signal reported for the GP32–ssDNA complex (Scheerhagen et al., 1985a; Kuil et al., 1990). If the orientation of a molecule is largely dominated by an induced dipole moment, as in the case of double-stranded DNA, the rise of the signal is symmetric with the decay of the signal. As the rise of the birefringence signal is almost symmetric with the decay for the SSB–DNA complex, the influence of a permanent dipole must be small. The absence of a significant permanent dipole moment is possibly related to the symmetry properties of the bound tetramer. On the other hand, due to a redistribution of charges upon complexation, a permanent dipole moment can be created. For the GP32–DNA complex, it was observed that both an induced and a permanent dipole moment are involved in the orientation of the complex (Scheerhagen et al., 1985a; Scheerhagen, 1986; Kuil et al., 1990).

*Dimensions of the SSB–DNA Complexes.* The electric field induced birefringence decay was analyzed to obtain the rotation diffusion coefficient of the SSB complexed with either the 145 bp or the 270 bp DNA fragment. The decay of the birefringence signal could not be described adequately with a single exponential. As mentioned above, we have used a double-exponential fit to obtain a slow and a fast decay time from the digitized signal (see Table I). The interpretation of this double-exponential signal is not straightforward. For the GP32–ssDNA complex, the double-exponential decay could be ascribed to rotational motion along the short axis of a

cylindrical particle, whereas similar observations with double-stranded DNA have been interpreted in terms of bending motions and flexibility. For GP32–ssDNA and GP32–tRNA complexes, the ratio of the slow relaxation time to the fast relaxation time ranged from 4.0 to 4.7, while for the SSB complexes the ratio of the fast and the slow decay times is typically a factor of 5–7. However, it should be noted that this ratio is more difficult to estimate accurately for the fast signals from SSB complexes than for the slower GP32 signals. Apart from the interpretation of the fast component, the slow phase in the decay of the electric birefringence signal can unequivocally be attributed to the end over end rotation of the molecule (Wegener et al., 1979). The value of the slow decay time obtained for both fragments can be used to calculate the length of a cylinder with the hydrodynamic dimensions of the molecule in solution, relatively independent of the actual radius of the cylinder (Tirado & de la Torre, 1980; Elias & Eden, 1981; Stellwagen, 1981; Hagerman, 1981). In this calculation, we assume that the diameter of the complex is determined by the diameter of a single tetramer (7.6–7.8 nm) (Weiner et al., 1975; Bandyopadhyay & Wu, 1978). Thus, we obtained for the 145 bp SSB complex a hydrodynamic length of 34 ± 2 nm, and for the 270 bp SSB complex a length of 59 ± 3 nm. These values correspond to apparent base–base distances of 0.24 ± 0.02 and 0.22 ± 0.03 nm for the short and larger complex, respectively, in rather good agreement with the electron microscopy estimates of 0.19 nm (Sigal et al., 1972). Since the base–base distances for the the 145 and 270 bp SSB complex are the same within experimental error, we must conclude that the rigid cylinder model is a reasonable hydrodynamic model for these complexes and that flexibility plays a minor role. In the case of GP32, the base–base distance was clearly different for complexes with 145 and 270 bp indicative of significant flexibility (Kuil et al., 1990). For SSB bound in the $n = 35$ mode to ssDNA, the structure of the complex is probably rather compact in view of the dimensions calculated for the complex, and possibly this compact structure is significantly more rigid than the GP32 complex. On the other hand, the total length of the complexes may be too short to observe significant flexibility using the field-free decay of the birefringence signal. In conclusion, the average value of 0.23 ± 0.03 nm for the projected base–base distance is a lower limit in view of the superhelical structure of the complex; the path of a DNA chain wrapped around a protein core is longer than the straight linear dimension of the hydrodynamic equivalent cylinder.

## Discussion

It seems likely that all the complexes between single-stranded DNA-binding proteins and single-stranded DNA are characterized by a rather large local base–base distance for the polynucleotide in the complex in view of the rather similar CD spectra obtained (Anderson & Coleman, 1975; Scheerhagen, 1986; van Amerongen et al., 1987). The ssDNA remains well organized in the complex, and the bases are tilted and twisted relative to the local helix axis, as was elegantly shown for the GP32–ssDNA and gene V–ssDNA complexes using linear dichroism spectroscopy (van Amerongen et al., 1988, 1990b; van Amerongen & van Grondelle, 1989). Moreover, an increased local base–base distance is characteristic for the complexed DNA (Scheerhagen, 1986; Scheerhagen et al., 1989; van Amerongen et al., 1987, 1990a,b; van Amerongen & van Grondelle, 1989). These properties may be related to the primary functions of these proteins: destabilizing double-helical hairpins, protection of single-stranded DNA from nucleases, and a positive stimulation of the cognate polymerase. Shifting the single-strand/double-strand equilibrium and organizing the nucleotides in a hydrophobic environment, suitable to enhance the polymerase action, are probably the most important functions of these proteins during DNA replication, apart from protecting the single-stranded DNA template from nucleases. The projected base–base distance observed in the electric birefringence experiment for the SSB–ssDNA complexes is in reasonable agreement with the value determined from electron microscopy experiments by Sigal et al. (1972). The use of electric birefringence decays to calculate the length of DNA complexes seems a reliable method to obtain the base–base distance in solution, even when the experiments are performed over a limited range of salt concentrations. It should be noted, however, that the binding properties of the associated proteins should be checked extensively in these low salt conditions, preferably both before and after the experiment. Especially in case of the SSB protein the binding properties should be monitored since otherwise a combination of binding modes might be studied. Fortunately, the low salt binding mode is stable over a considerable traject of salt concentrations. On the other hand, the experimental limitations due to the use of an electric field to orient the complex prevent study of the high salt binding mode, although possibly carefully designed experiments can be performed using Mg-containing buffers that induce the high salt binding mode at lower ionic strength.

The positive birefringence signal can be related to a substantial tilt of the bases if the orientation of the complex is along the long particle axis. The occurrence of a biphasic decay of the birefringence signal might be an indication for rotation around the short axis of the complex as suggested for GP32–DNA complexes (Scheerhagen, 1986; Kuil et al., 1990). In view of the time resolution of the present electric birefringence setup, it is rather speculative to analyze the time constants of the fast components observed in the birefringence decay. Transient photodichroism experiments that are being performed currently in our laboratory are aimed at the determination of the size of the different single-stranded DNA-binding proteins and have a much better time resolution that hopefully leads to further insight in the solution structure and dynamics of these proteins both free and in complexes with DNA and RNA.

## Acknowledgments

We thank Dr. J. A. Brandsma and Prof. P. van der Putte (State University, Leiden, The Netherlands) for providing the *E. coli* strain carrying the temperature-inducible plasmid for the overproduction of SSB protein. The expert technical assistance of J. den Blaauwen during the preparation of the nucleosomal DNA fragments is highly appreciated. Fruitful discussions with Dr. H. van Amerongen are gratefully acknowledged.

**Registry No.** Poly(rA), 24937-83-5.

## References

Anderson, R. A., & Coleman, J. E. (1975) *Biochemistry 14*, 5485–5491.

Bandyopadhyay, P. K., & Wu, C. W. (1978) *Biochemistry 17*, 4078–4085.

Bokma, J. T., Johnson, W. C., Jr., & Blok, J. (1987) *Biopolymers 26*, 893–909.

Bradford, M. M. (1976) *Anal. Biochem. 72*, 248–254.

Brandsma, J. A., van Sluis, C. A., & van de Putte, P. (1981) *J. Bacteriol. 147*, 682–684.

Bujalowski, W., & Lohman, T. M. (1986) *Biochemistry 25*, 7799–7802.

Bujalowski, W., & Lohmann, T. M. (1987) *J. Mol. Biol. 195*, 897–907.
Bujalowski, W., Overman, L. B., & Lohman, T. M. (1988) *J. Biol. Chem. 263*, 4629–4640.
Chase, J. W., & Williams, K. R. (1986) *Annu. Rev. Biochem. 55*, 103–136.
Delius, H., Mantell, N. J., & Alberts, B. (1972) *J. Mol. Biol. 67*, 341.
Elias, J. G., & Eden, D. (1981) *Macromolecules 14*, 410.
Greve, J. (1972) Ph.D. Thesis, Free University Amsterdam.
Hagerman, P. (1981) *Biopolymers 20*, 1503.
Kowalczykowski, S. C., & Krupp, R. A. (1987) *J. Mol. Biol. 193*, 97–113.
Kowalczykowski, S. C., Leland, S. P., Lonberg, N., Newport, J. W., McSwiggen, J. A., & von Hippel, P. H. (1986) *Biochemistry 25*, 1226–1240.
Kowalczykowski, S. C., Clow, J., Somani, R., & Varghese, A. (1987) *J. Mol. Biol. 193*, 81–95.
Kuil, M. E., van Mourik, F., Burger, W., & van Grondelle, R. (1988) *Biophys. Chem. 32*, 211–227.
Kuil, M. E., van Amerongen, H., van der Vliet, P. C., & van Grondelle, R. (1989) *Biochemistry 28*, 9795–9800.
Kuil, M. E., van der Oord, C. J. R., Vlaanderen, C. A., van Haeringen, B., & van Grondelle, R. (1990) *J. Biomol. Struct. Dyn. 7*, 943–957.
Lohman, T. M., & Overman, L. (1985) *J. Biol. Chem. 260*, 3594–3603.
Lohman, T. M., Green, J. M., & Beyer, R. S. (1986) *Biochemistry 25*, 21–25.
Lohman, T. M., Bujalowski, W., & Overman, L. (1988) *Trends Biochem. Sci. (Pers. Ed.) 13*, 250.
Low, R. L., Shlomai, J., & Kornberg, A. (1982) *J. Biol. Chem. 257*, 6242.
Lutter, L. C. (1978) *J. Mol. Biol. 124*, 391–420.
Marquardt, D. W. (1963) *J. Soc. Ind. Appl. Math. 11*, 431.
McGhee, J. D., & von Hippel, P. H. (1974) *J. Mol. Biol. 86*, 469.
Molineux, I. J., & Gefter, M. L. (1975) *J. Mol. Biol. 98*, 811.
Morrical, S. W., Lee, J., & Cox, M. M. (1986) *Biochemistry 25*, 1482.
Scheerhagen, M. A. (1986) Ph.D. Thesis, Free University Amsterdam.
Scheerhagen, M. A., van Amerongen, H., van Grondelle, R., & Blok, J. (1985a) *FEBS Lett. 179*, 221.
Scheerhagen, M. A., Kuil, M. E., van Grondelle, R., & Blok, J. (1985b) *FEBS Lett. 184*, 221.
Scheerhagen, M. A., Bokma, J. T., Vlaanderen, C. A., Blok, J., & van Grondelle, R. (1986a) *Biopolymers 25*, 1419–1448.
Scheerhagen, M. A., Vlaanderen, C. A., Blok, J., & van Grondelle, R. (1986b) *J. Biomol. Struct. Dyn. 3*, 887–898.
Scheerhagen, M. A., Kuil, M. E., van Amerongen, H., & van Grondelle, R. (1989) *J. Biomol. Struct. Dyn. 6*, 701–706.
Sigal, N., Delius, H., Kornberg, T., Gefter, M. L., & Alberts, B. (1972) *Proc. Natl. Acad. Sci. U.S.A. 69*, 3536–3541.
Stellwagen, N. C. (1981) *Biopolymers 20*, 399.
Tirado, M., & Garcia de La Torre, J. (1980) *J. Chem. Phys. 73*, 1986–1993.
van Amerongen, H. (1989) Ph.D. Thesis, Free University Amsterdam.
van Amerongen, H., & van Grondelle, R. (1989) *J. Mol. Biol. 209*, 433–445.
van Amerongen, H., van Grondelle, R., & van der Vliet, P. C. (1987) *Biochemistry 26*, 4646–4652.
van Amerongen, H., Kuil, M. E., van Mourik, F., & van Grondelle, R. (1988) *J. Mol. Biol. 204*, 397–405.
van Amerongen, H., Kuil, M. E., Scheerhagen, M. A., & van Grondelle, R. (1990a) *Biochemistry 29*, 5619–5625.
van Amerongen, H., Kwa, S., & van Grondelle, R. (1990b) *J. Mol. Biol.* (submitted for publication).
Wegener, W. A., Dowben, R. M., Koester, V. A. (1979) *J. Chem. Phys. 70*, 622.
Weiner, J. H., Bertsch, L. L., & Kornberg, A. (1975) *J. Biol. Chem. 250*, 1972–1980.